CRYSTAL GROWTH & DESIGN
2009
VOL. 9, NO. 1
368–371

Hydrothermal Syntheses, Crystal Structure, and Magnetic Characterization of Two 3d-4f Heterometallic Coordination Polymers

Ning Wang,[†] Shantang Yue,*[,†] Yingliang Liu,[‡] Haiyu Yang,[†] and Hongyan Wu[†]

School of Chemistry and Environment, South China Normal University, Guangzhou 510006, P. R. China, and School of Chemistry, Jinan University, Guangzhou 510006, P. R. China

Received June 3, 2008; Revised Manuscript Received September 4, 2008

ABSTRACT: Two 3d-4f heterometallic coordination polymers, $[Gd^{III}_2Cu^{II}(pydc)_2(CO_3)_2(H_2O)_2]\cdot 2H_2O$ (**1**, pydc = 2,5-pyridinedicarboxylate dianion) and $[Gd^{III}_4Co^{II}Co^{III}(\mu_3\text{-}OH)_3(\mu_3\text{-}O)(pydc)_6(H_2O)_5]\cdot 8H_2O$ (**2**) have been synthesized under hydrothermal conditions. In compound **1**, 2D $\{[Gd_2(CO_3)_2]^{2+}\}_n$ sheets are connected by $[Cu(pydc)_2]^{2-}$ bridges, which give rise to the formation of a sandwich-like framework. Compound **2** exhibits a 3D framework constructed by Gd_4 clusters, Co_2 subunits, and pydc spacers. The solid-state dc magnetic measurements reveal antiferromagnetic behaviors of **1** and **2** in both compounds.

Introduction

The design and synthesis of 3d-4f heterometallic coordination polymers have been of increasing interest.[1] The intense interest in this field is justified not only by the intriguing structural diversity of the polymer architectures but also by the potential applications of these compounds as functional materials in magnetism,[2] molecular adsorption,[3] manufacture of light conversion devices,[4] and bimetallic catalysis.[5] Although a number of 3d-4f heterometallic compounds have been synthesized and characterized,[6] the frameworks based on combination of CO_3^{2-} and 2,5-pyridinedicarboxylate dianion (pydc) connections or mixed μ_3-OH^-, μ_3-O^{2-}, and pydc bridges are rarely reported.[7] In recent years, because of high efficiency and the easy operation, hydrothermal synthesis has been widely used in the self-assembly of coordination polymers.[8] Furthermore, the thermally stable compounds are usually obtained from a hydrothermal reaction system.[9] With this in mind, we used pydc and oxalate anions as mixed ligands to assemble 3d-4f coordination polymers. Herein, we report the hydrothermal synthesis, crystal structure, and magnetic properties of two novel 3d-4f coordination polymers $[Gd^{III}_2Cu^{II}(pydc)_2(CO_3)_2(H_2O)_2]\cdot 2H_2O$ (**1**) and $[Gd^{III}_4Co^{II}Co^{III}(\mu_3\text{-}OH)_3(\mu_3\text{-}O)(pydc)_6(H_2O)_5]\cdot 8H_2O$ (**2**).

Experimental Section

General Procedures. Both compounds were synthesized under hydrothermal conditions in 23 mL Teflon-lined Parr autoclaves. Starting materials include copper chloride hexahydrate ($CuCl_2\cdot 6H_2O$, 99%, Alfa-Aesar), cobalt chloride hexahydrate ($CoCl_2\cdot 6H_2O$, 99%, Alfa-Aesar), 2,5-pyridinedicarboxylic acid (H_2pydc, Alfa-Aesar), potassium oxalate hydrate ($K_2(C_2O_4)\cdot H_2O$, 99%, Alfa-Aesar), and triethylamine (Alfa-Aesar). It was found that the CO_3^{2-} dianions were formed during the hydrothermal synthesis of compound **1**, which may be attributed to the cleavage of C−C bonds and the oxidation of oxalate ligands. After reaction, the products were filtered, washed with deionized water, and dried in air.

The C, H, and N microanalysis were carried out with Perkin-Elmer 240 elemental analyzer. The FT-IR spectra were recorded from KBr pellets in the 4000−400 cm^{-1} ranges on a Nicolet 5DX spectrometer. Thermogravimetric (TG) analysis of compound **2** was performed at a rate of 10 °C/min under N_2 using a NETZSCH TG 209 system. The magnetic susceptibility measurements for **1** and **2** were carried out on polycrystalline samples on a Quantum Design MPMS-XL5 SQUID magnetometer in the temperature range of 2−300 K. Diamagnetic corrections were estimated from Pascal's constants for all constituent atoms.

Hydrothermal Synthesis of $[Gd^{III}_2Cu^{II}(pydc)_2(CO_3)_2(H_2O)_2]\cdot 2H_2O$ (1). $Gd(NO_3)_3\cdot 6H_2O$ (0.23 g, 0.5 mmol), $CuCl_2\cdot 6H_2O$ (0.12 g, 0.5 mmol), $K_2(C_2O_4)\cdot H_2O$ (0.09 g, 0.5 mmol), H_2pydc (0.17 g, 1 mmol), and triethylamine (0.03 g, 0.3 mmol) were added to water (10 g, 556 mmol). The mixture was added to a 15 mL Teflon-lined autoclave. After heating at 443 K for three days and then cooling to room temperature in air, blue block-like crystals of compound **1** could be isolated in ∼75% yield. Anal. Calcd for $C_{16}H_{14}CuGd_2N_2O_{18}$: C, 21.34; H, 1.57; N, 3.11. Found: C, 21.31; H, 1.51; N, 3.15. IR (KBr, cm^{-1}): 3498(s), 2250(w), 1750(s), 1400(m), 1250(w), 900(m), 650(m).

Hydrothermal Synthesis of $[Gd^{III}_4Co^{II}Co^{III}(\mu_3\text{-}OH)_3(\mu_3\text{-}O)(pydc)_6(H_2O)_5]\cdot 8H_2O$ (2). $Gd(NO_3)_3\cdot 6H_2O$ (0.23 g, 0.5 mmol), $CoCl_2\cdot 6H_2O$ (0.12 g, 0.5 mmol), H_2pydc (0.17 g, 1 mmol), and triethylamine (0.03 g, 0.3 mmol) were added to water (10 g, 556 mmol). The mixture was added to a 15 mL Teflon-lined autoclave in argon atmosphere. After heating at 443 K for three days and then cooling to room temperature in air, blue block-like crystals of compound **1** could be isolated in ∼60% yield. Anal. Calcd for $C_{42}H_{32}Co_2Gd_4N_6O_4$: C, 35.24; H, 2.25; N, 5.87. Found: C, 35.21; H, 2.27; N, 5.84. IR (KBr, cm^{-1}): 3750(w), 2900(m), 2425(w), 1750(m), 1400(w), 1250(w), 1000(s), 750(s).

Crystallographic Data Collection and Refinement. Crystal data and details of the data collection and refinement for **1** and **2** are summarized in Table 1. The selected bond lengths and bond angles are listed in Table S1 and S2, Supporting Information. X-ray diffraction data were recorded on a Bruker SMART Apex CCD system with graphite-monochromated Mo Kα radiation (λ = 0.71073 Å) at 298 K. Absorption corrections were applied by SADABS. The structures were solved by direct methods and refined by full-matrix least-squares techniques on F^2 using the SHELXTL[10] program package. All nonhydrogen atoms were refined with anisotropic displacement parameters.

Results and Discussion

Structure Description of 1. The crystal structure of compound **1** is depicted in Figure 1. Compound **1** contains coordinated CO_3^{2-} dianions, which may be incorporated from the decomposition and oxidation of oxalate ligands. The asymmetric unit consists of one unique Cu^{II}, two crystallographically independent Gd^{III} metal centers, two pydc dianions, two coordinated CO_3^{2-} dianions, two coordinated aqueous ligands, and two free water molecules. Cu1 is five-coordinate with a lengthened tetragonal pyramid coordination environment which is fulfilled by two N atoms (N1, N2) and three O atoms

* To whom correspondence should be addressed. E-mail: yuesht@scnu.edu.cn. Fax: 86 20-39310187.
[†] South China Normal University.
[‡] Jinan University.

10.1021/cg800575f CCC: $40.75
Published on Web 11/17/2008

Table 1. Crystal Data and Structure Refinement for 1 and 2

	1	2
empirical formula	$C_{16}H_{14}CuGd_2N_2O_{18}$	$C_{42}H_{32}Co_2Gd_4N_6O_{41}$
formula mass	900.34	2023.60
T (K)	296(2)	296(2)
wavelength (Å)	0.71073	0.71073
cryst syst	monoclinic	triclinic
space group	$P21$	$P\bar{1}$
a (Å)	9.56440(10)	11.9248(2)
b (Å)	7.84380(10)	16.1606(3)
c (Å)	15.51580(10)	17.5254(3)
α (deg)	90	90.0880(10)
β (deg)	102.0100(10)	98.5630(10)
γ (deg)	90	109.9390(10)
V (Å^3)	1138.54(2)	3134.53(10)
Z	2	2
D_{calcd} (g cm^{-3})	2.626	2.144
μ (mm^{-1})	6.780	4.797
$F000$	850.0	1928.0
data/restraints/params	5023/13/376	14191/4/868
GOF on F^2	0.945	1.011
$R_1{}^a$ [$I > 2\sigma(I)$]	0.0287	0.0482
$\omega R_2{}^b$	0.0579	0.0981
largest diff peak and hole (e Å^{-3})	1.608 and >−1.043	1.216 and −1.309

^{a} $R_1 = \Sigma[||F_0| - |F_c||]/\Sigma|[F_0|$ ^{b} $[\omega R_2 = [\Sigma[\omega(F_0^2 - F_c^2)^2]/\Sigma[\omega(F_0^2)^2]]^{1/2}$.

(O10, O11, O9#1; #1 = 1 − x, −1/2 + y, 1 − z) donated by three different pydc ligands, where O9#1 locates the four-fold axis position with a bond distance of 2.63 Å for Cu1−O9#1, larger than the normal 1.99 Å of Cu−O for a six-coordinate Cu^{II} cation, which reveals the distinct Jahn−Teller effect. N1, N2 and O10, O11 occupy the trans-sites of the plane with N2−Cu1−N1 = 175.4(2)°, O11−Cu1−O10 = 178.8(2)°, respectively. Both of Gd1 and Gd2 are nine-coordinate with a triaugmented triangular prism coordination polyhedron. Gd1 and Gd2 have the same coordination environment which is completed by six CO_3^{2-}-O, two pydc-O, and one aqua-O atoms. The Gd−O bond distances for Gd1 and Gd2 fall in the range of 2.33−2.52 Å and 2.34−2.63 Å, respectively. Gd1 and Cu1 are bridged by one pydc ligand with Gd1···Cu1 = 8.68(5) Å. Gd1 and Gd2 are connected by two CO_3^{2-} anions with Gd1···Gd2 = 4.71(2) Å (Figure 1a). As shown in Figure 1b, along b-axis direction, a three-dimensional sandwich-like packing structure is constructed from $\{[Gd_2(CO_3)_2]^{2+}\}_n$ sheets and $[Cu(pydc)_2]^{2-}$ bridges, where the Gd−Gd separation based on CO_3^{2-} connections is 4.12 and 4.85 Å. It is of interest that the adjacent $[CuO_3N_2]$ lengthened tetragonal pyramids point to the opposite directions. As a result, the copper zigzag chains are formed in turn in the ABAB-type sandwich-like 3D networks as shown in Figure 1c (copper chains are represented by red zigzag curves, the 2D gadolinium sheets are symbolized by black networks).

Structure Description of 2. The structure of compound **2** is displayed in Figure 2. The guest−water-free asymmetric unit of compound **2** contains four Gd^{III}, one Co^{II}, one Co^{III} mental centers, six pydc ligands, three μ_3-OH^-, one μ_3-O^{2-} anions, and five coordinated water molecules. The two Co atoms(Co1, Co2) contained in the crystal structure exhibit two different oxidation states (+2 for Co1 and +3 for Co2). However, there is no Co^{III} salt in the starting material. The higher oxidation state for Co2 can be proved by the shorter Co−O and Co−N bond distance for Co2 than that for Co1 (1.913−1.934 Å and 1.957−1.982 Å for Co2, 2.074−2.123 Å and 2.088−2.154 Å for Co1), and it is further demonstrated by the BVS[11] calculating results. The formation of Co^{III} cation may be attributable to the hydrothermal oxidation of the Co^{II} cation existing in the starting material. As shown in Figure 2a, the four crystallographically independent Gd atoms (Gd1, Gd2, Gd3, Gd4) are connected by one μ_3-O^{2-}-O(O2) and three μ_3-OH^--O(O1,O3,O4) atoms,

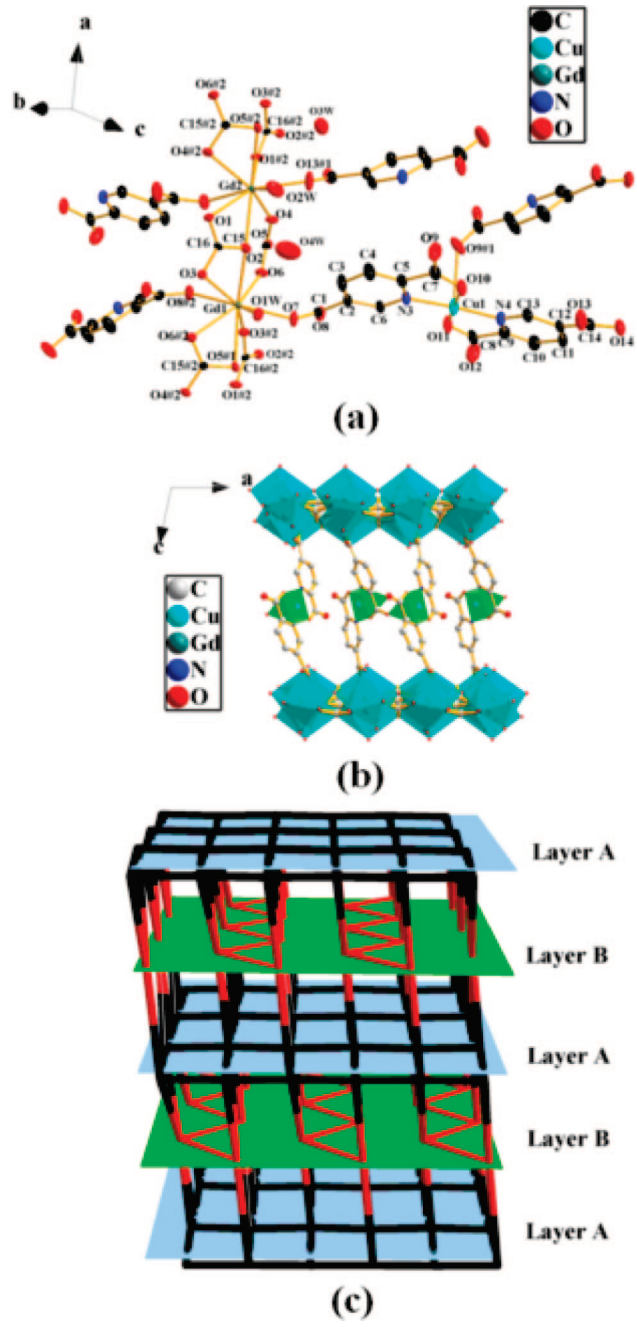

Figure 1. (a) View of the asymmetric unit of **1**. (b) Diagram showing the stacked sandwich-like framework along b-axis. The coordination polyhedrons of Gd and Cu atoms are represented. (c) View of the ABAB-type 3D sandwich-like packing structure of **1**. Red rods represent the copper zigzag chains; the 2D gadolinium sheets are symbolized by black networks. Symmetric codes: #1 = −x, 1/2 + y, −z; #2 = 1 − x, −1/2 + y, −z.

which gives rise to the formation of a Gd_4 cluster, where the Gd···Gd separation ranges from 3.67 to 3.91 Å. We can also find that there are three different coordination environments for the four Gd atoms, where Gd2 and Gd3 have the same coordination sphere (the complete coordination environments for Gd1−Gd4 can be seen in Figure S1−S3 in Supporting Information). Gd1 is nine-coordinated with three μ_3-OH^--O, one aqua-O, and five pydc-O atoms. Gd2 is eight-coordinated with two μ_3-OH^--O, one μ_3-O^{2-}-O, two aqua-O, and three pydc-O atoms. Gd4 is eight-coordinated with one pydc-N, one μ_3-OH^--O, one μ_3-O^{2-}-O, and five pydc-O atoms. The coordination environment of Co1 is different from that of Co2, where

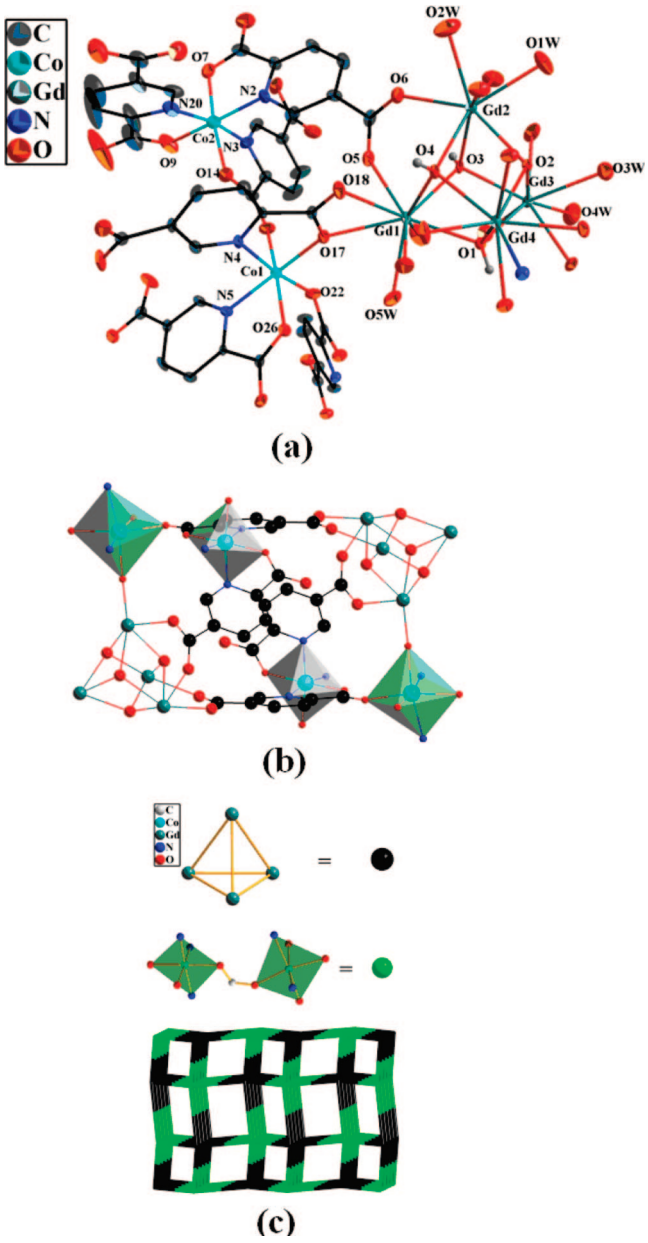

Figure 2. (a) View of the guest−water-free asymmetric unit of **2**. (b) Diagram showing the closed ring of $Gd_4-Co_2-Gd_4-Co_2-Gd_4$. The coordination polyhedrons of Co atoms are represented. (c) View of the three-dimensional framework of **2**. Gd_4 clusters are simplified to black dots; Co_2 units are represented by green dots.

Co1 is six-coordinated with two pydc-N and four pydc-O atoms while Co2 is six-coordinated with three pydc-N and three pydc-O atoms. One closed ring of $Gd_4-Co_2-Gd_4-Co_2-Gd_4$ has been shown in Figure 2b, where every part is connected to each other via pydc bridge. It is intriguing that a three-dimensional framework based on black Gd_4 and green Co_2 nodes can be displayed as shown in Figure 2c.

TG Analyses. To examine the thermal stability of compound **2**, thermal gravimetric (TG) analysis was carried out (see Supporting Information, Figure S4). The TG curve of **2** shows a total weight loss of 11.35% in the range of 25−360 °C (calcd 11.56%), which corresponds to the loss of all noncoordinated and coordinated water molecules.

Magnetic Property of 1. Solid-state dc magnetic susceptibility measurement for compound **1** was performed in the range of 2−300 K under a field of 500 Oe, and the magnetic behavior

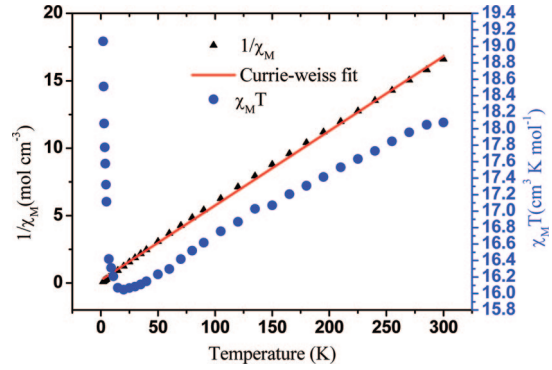

Figure 3. $1/\chi_M$ vs T and $\chi_M T$ vs T plots for compound **1**.

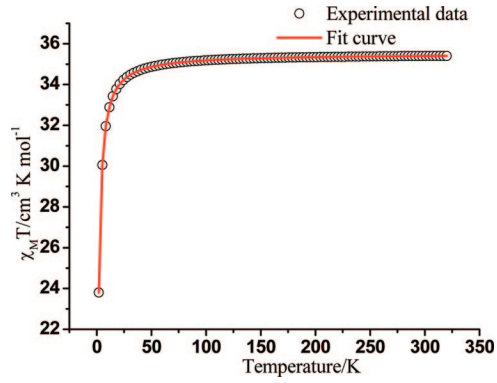

Figure 4. $\chi_M T$ vs T plots for compound **2**. The dots represent the experimental data, and the solid lines represent the best fitting data which were calculated with the method as shown in the text.

is shown in Figure 3, as plots of $1/\chi_M$ versus T and $\chi_M T$ versus T, where χ_M is the magnetic susceptibility per $[Gd_2Cu]$ unit. The room-temperature $\chi_M T$ value is 18.08 $cm^3 \cdot K \cdot mol^{-1}$, higher than the spin-only value 16.13 $cm^3 \cdot K \cdot mol^{-1}$ for two Gd^{III} ($S = 7/2$) and one Cu^{II} ($S = 1/2$) paramagnetic cations with an average $g = 2$. As the temperature lowered from 300 to 20 K, the $\chi_M T$ value decreased steadily from 18.08 $cm^3 \cdot K \cdot mol^{-1}$ to 16.05 $cm^3 \cdot K \cdot mol^{-1}$. But along with the temperature continuously lowering to 2 K, the $\chi_M T$ value abruptly increased to 19.06 $cm^3 \cdot K \cdot mol^{-1}$, indicating that the antiferromagnetic coupling between Gd^{III} and Cu^{II} ions leads to the ferrimagnetic behavior in this compound. The $1/\chi_M$ data obeys Curie−Weiss Law, $\chi = C/(T - \theta)$, with a Curie constant $C = 18.07$ $cm^3 \cdot K \cdot mol^{-1}$ and a negative Weiss constant $\theta = -3.96$ K. The negative Weiss constant also gives the evidence of antiferromagnetic interactions existing in compound **1**.

Magnetic Property of 2. Solid-state dc magnetic susceptibility measurement for compound **2** was performed in the range of 2−300 K under a field of 4 kOe, and the magnetic behavior is shown in Figure 4 as plots of $\chi_M T$ versus T, where χ_M is the magnetic susceptibility per $[Gd_4Co_2]$ unit. The room-temperature $\chi_M T$ value is 35.39 $cm^3 \cdot K \cdot mol^{-1}$, much higher than the spin-only value 33.375 $cm^3 \cdot K \cdot mol^{-1}$ for four Gd^{III} ($S = 7/2$, assuming $g_{Gd} = 2.0$), one high-spin Co^{II} ($S = 3/2$, assuming $g_{Co} = 2$), and one low-spin Co^{III} ($S = 0$) cations, indicating the significant orbital contribution of Co^{II} ion in this compound. As the temperature lowered from 300 to 2 K, the $\chi_M T$ value decreased steadily from 35.39 $cm^3 \cdot K \cdot mol^{-1}$ to 23.80 $cm^3 \cdot K \cdot mol^{-1}$, which reveals an overall antiferromagnetic behavior in compound **2**. Because of the complicated three-dimensional framework of **2**, no exact theoretical expression could be used to simulate the magnetic data. Therefore, we

assumed that one isolated high-spin Co^{II} cation and one Gd_4 cluster contributed to the magnetic susceptibility of the $[Gd_4Co_2]$ unit. In addition, the magnetic interactions between Gd atoms in the Gd_4 cluster were regarded as the same for further simplification. Based on Van-Vleck equation, the expression for magnetic susceptibility per $[Gd_4Co_2]$ unit can be deduced as below. The best fitting parameters are $g_{Co} = 2.30(4)$, $g_{Gd} = 2.09(2)$, $J = -0.02(1)$ cm^{-1}. The small negative value of J reveals weak antiferromagnetic interactions in the Gd_4 cluster.

$$\chi_M = \chi_{Co(II)} + \chi_{Gd\text{-}cluster}$$

$\chi_{Co(II)} = Ng_{Co}^2\beta^2/(3k_BT)S_{Co}(S_{Co} + 1)$, $\chi_{Gd\text{-}cluster} = Ng_{Gd}^2\beta^2/(3k_BT)A/B$, where $A = 126\exp(2J/k_BT) + 930\exp(6J/k_BT) + 3192\exp(12J/k_BT) + 7560\exp(20J/k_BT) + 14190\exp(30J/k_BT) + 22386\exp(42J/k_BT) + 34272\exp(56J/k_BT) + 34272\exp(72J/k_BT) + 35910\exp(90J/k_BT) + 34650\exp(110J/k_BT) + 27830\exp(121J/k_BT) + 11232\exp(156J \times /k_BT) + 14742\exp(182J/k_BT) + 6090\exp(210J/k_BT)$, and $B = 8 + 63\exp(2J/k_BT) + 155\exp(6J/k_BT) + 266\exp(12J/k_BT) + 378\exp(20J/k_BT) + 473\exp(30J/k_BT) + 533\exp(42J/k_BT) + 612\exp(56J/k_BT) + 476\exp(72J/k_BT) + 399\exp(90J/k_BT) + 315\exp(110J/k_BT) + 230\exp(121J/k_BT) + 72\exp(156J/k_BT) + 81\exp(182J/k_BT) + 29\exp(210J/k_BT)$.

Conclusion

In this paper, two new 3d-4f coordination polymers were successfully synthesized by applying hydrothermal strategy. The transformation of oxalate to carbonate in **1**, and the hydrothermal oxidation in **2**, proved that the hydrothermal process is indeed hard to predict and not easy to control. The sandwich-like framework of **1**, constructed by $\{[Gd_2(CO_3)_2]^{2+}\}_n$ sheets and $[Cu(pydc)_2]^{2-}$ bridges, and the three-dimensional metal−organic framework of **2**, assembled by Gd_4 cluster, Co_2 subunit, and pydc spacers, are all of interest. The successful assembly of the two compounds may be of use for the application of hydrothermal strategy in constructing high dimensional coordination polymers.

Acknowledgment. This work was financially supported by Nature and Science Foundation of Guangdong Province (Grant 7005808), Guangdong Provincial Science and Technology Bureau (2008B010600009), and NSFC (Grant U0734005).

Supporting Information Available: Selected geometric information for **1** and **2**, coordination geometries of metal ions, TG curves for **2** and X-ray data files in CIF format. This material is available free of charge via the Internet at http://pubs.acs.org.

References

(1) (a) He, Z.; He, C.; Gao, E. Q.; Wang, Z. M.; Yang, X. F.; Liao, C. S.; Yan, C. H. *Inorg. Chem.* **2006**, *42*, 2206. (b) Yamaguchi, T.; Sunatsuki, Y.; Kojima, M.; Akashi, H.; Tsuchimoto, M.; Re, N.; Osa, S.; Matsumoto, N. *Chem. Commun.* **2004**, *9*, 1048. (c) Yukawa, Y.; Aromi, G.; Igarashi, S.; Ribas, J.; Zvyagin, S. A.; Krzystek, J. *Angew.Chem., Int.Ed.* **2005**, *44*, 1997. (d) Liang, Y. C.; Cao, R.; Su, W. P.; Hong, M. C.; Zhang, W. J. *Angew. Chem., Int. Ed.* **2000**, *39*, 3304. (e) Cutland, A. D.; Malkani, R. G.; Kampf, J. W.; Pecoraro, V. L. *Angew. Chem., Int. Ed.* **2000**, *39*, 2689. (f) Kou, H. Z.; Jiang, Y. B.; Cui, A. L. *Cryst. Growth Des.* **2005**, *5*, 77. (g) Costes, J. P.; Novitchi, G.; Shova, S.; Dahan, F.; Donnadieu, B.; Tuchagues, J. P. *Inorg. Chem.* **2004**, *43*, 7792. (h) Bencini, A.; Benelli, C.; Caneschi, A.; Dei, A.; Gatteschi, D. *Inorg. Chem.* **1986**, *25*, 572.

(2) (a) Chen, W. T.; Wang, M. S.; Cai, L.; Xu, G.; Akitsu, T.; Motoko, A. T.; Guo, G. C.; Huang, J. S. *Cryst. Growth Des.* **2006**, *6*, 1738. (b) Aronica, C.; Chastanet, G.; Pilet, G.; Guennic, B.; Robert, L. V.; Wernsdorfer, W.; Luneau, D. *Inorg. Chem.* **2007**, *46*, 6108. (c) Okazawa, A.; Nogami, T.; Nojiri, H.; Ishida, T. *Chem. Mater.* **2008**, *20*, 3110. (d) Zhang, J. J.; Hu, S. M.; Xiang, S. C.; Sheng, T. L.; Wu, X. T.; Li, Y. M. *Inorg. Chem.* **2006**, *45*, 7173. (e) Chandrasekhar, V.; Pandian, B. M.; Boomishankar, R.; Steiner, A.; Vittal, J. J.; Houri, A.; Clerac, R. *Inorg. Chem.* **2008**, *47*, 4919. (f) Liu, F. C.; Zeng, Y. F.; Jiao, J.; Li, J. R.; Bu, X. H.; Ribas, J.; Batten, S. R. *Inorg. Chem.* **2006**, *45*, 6129.

(3) (a) Zhao, B.; Cheng, P.; Dai, Y.; Cheng, C.; Liao, D. Z.; Yan, S. P.; Jiang, Z. H.; Wang, G. L. *Angew. Chem., Int. Ed.* **2003**, *42*, 934. (b) Zhao, B.; Cheng, P. X.; Chen, Y.; Cheng, C.; Shi, W.; Liao, D. Z.; Yan, S. P.; Jiang, Z. H. *J. Am. Chem. Soc.* **2004**, *126*, 3012.

(4) (a) Zhao, B.; Chen, X. Y.; Cheng, P.; Liao, D. Z.; Yan, S. P.; Jiang, Z. H. *J. Am. Chem. Soc.* **2004**, *126*, 15394. (b) Blasse, G. *Mater. Chem. Phys.* **1992**, *31*, 3. (c) Sabatini, N.; Guardigli, M.; Lehn, J. M. *Coord. Rev.* **1993**, *123*, 201.

(5) (a) Deng, H.; Shore, S. G. *J. Am. Chem. Soc.* **1991**, *113*, 8538. (b) Deng, H.; Chun, S.; Florian, P.; Grandinetti, P. J.; Sore, S. G. *Inorg. Chem.* **1996**, *35*, 3891.

(6) (a) Shutaro, O.; Takafumi, K.; Naohide, M.; Nazzareno, R.; Andrzej, P.; Jerzy, M. *J. Am. Chem. Soc.* **2004**, *126*, 420. (b) Valeriu, M. M.; Ayuk, M. A.; Rodolphe, C.; Wolfgang, W.; George, F.; Juan, B.; Christopher, E. A.; Annie, K. P. *J. Am. Chem. Soc.* **2007**, *129*, 9248. (c) Ren, P.; Shi, W.; Cheng, P. *Growth Des.* **2008**, *8*, 1097.

(7) (a) Chang, C. A.; Francesconi, L. C.; Malley, M. F.; Kumar, K.; Gougoutas, J. Z.; Tweedle, M. F.; Lee, D. W.; Wilson, L. J. *Inorg. Chem.* **1993**, *32*, 3501. (b) Shima, T.; Hou, Z. M. *J. Am. Chem. Soc.* **2006**, *128*, 8124.

(8) liang, Y. C.; Cao, R.; Su, W. P.; Hong, M. C.; Zhang, W. J. *Angew. Chem., Int. Ed.* **2000**, *39*, 3304.

(9) Wan, Y. H.; Zhang, L. P.; Jin, L. P.; Gao, S.; Lu, S. Z. *Inorg. Chem.* **2003**, *42*, 4985.

(10) (a) Sheldrick, G. M. SHELXL97, Program for Crystal Structure Refinement, Germany, 1997. (b) Sheldrick, G. M. *Acta Crystallogr., Sect. A: Found. Crystallogr.* **1990**, *46*, 467.

CG800575F